Applied Catalysis A, General 608 (2020) 117871

Contents lists available at ScienceDirect

Applied Catalysis A, General

journal homepage: www.elsevier.com/locate/apcata

Sustainable acrolein production from bio-alcohols on spinel catalysts: Influence of magnesium substitution by various transition metals (Fe, Zn, Co, Cu, Mn)

Vincent Folliard[a], Georgeta Postole[a], Livia Marra[b], Jean-Luc Dubois[c], Aline Auroux[a,*]

[a] Université de Lyon, Université Claude Bernard Lyon1, CNRS, IRCELYON, 2 avenue Albert Einstein, F- 69626, Villeurbanne Cedex, France
[b] BAIKOWSKI, 1046 Route de Chaumontet, F-74330 Poisy, France
[c] ARKEMA Direction Recherche & Développement, 420 Rue d'Estienne d'Orves, F-92705, Colombes, France

ARTICLE INFO

Keywords:
Alcohols oxidative coupling
Aldehydes co-adsorption
Adsorption microcalorimetry
Acid-base properties
FT-IR spectroscopy
Acrolein production

ABSTRACT

Acrolein is a widely used intermediate of synthesis for value-added compounds in a number of domains of application. This work reports on the sustainable synthesis of acrolein by oxidative coupling of bio-alcohols, which constitutes a very promising alternative to fossil fuel-based production. The synthesis is performed in two sequential reactors, using an iron molybdate catalyst for oxidation and then a magnesium aluminate spinel where magnesium is partly or totally substituted by transition metals (Fe, Zn, Co, Cu, Mn) as a catalyst for cross-aldolization. The acid-base properties of the latter catalysts were determined using SO_2 and NH_3 adsorption microcalorimetry. Adsorption microcalorimetry was also used to study the adsorption properties of the reactants, with formaldehyde, acetaldehyde and propionaldehyde as probe molecules, and was complemented by a FT-IR investigation of reactant adsorption in order to better understand the mechanisms of adsorption and reaction. Acrolein production was found to be correlated to the ionic radius of the transition metals used in the catalysts, indicating that electronic effects are likely a factor influencing the acrolein production.

1. Introduction

The reality of climate change and the means of addressing it, as surveyed in a comprehensive manner by the recent report of the IPCC (International Panel on Climate Change) [1], require a broad redesign of current practices with a new focus on sustainability. Some of the recommendations concern the use of sustainable bio-based feedstocks in the chemical industry, as a replacement for petroleum-based feedstocks and chemicals. A number of chemicals have already been studied in order to identify alternative processes using bio-based feedstocks/molecules. Among them, acrolein (propenaldehyde) has attracted attention as a promising target.

Discovered in 1893, acrolein, also known as propenal or acrylaldehyde, is the first of the unsaturated aldehyde series. Toxic, flammable, colorless and volatile, acrolein exhibits an acrid, unpleasant and irritating smell from which it takes its name [2]. Despite this, acrolein, with its conjugated vinyl and aldehyde groups, is a commonly used intermediate substance for the synthesis of a wide range of chemicals. One major application of acrolein is the production of acrylic acid which is a very important compound for the synthesis of polymers, superabsorbents, adhesives or inks [3–5]. Other applications include the production of D,L methionine, an essential amino-acid in animals feeds. Acrolein can also be used to produce water treatment chemicals or directly as a biocide to control the growth of aquatic weeds or algae and mollusks in water systems [2,3].

The first commercial synthesis of acrolein was performed by Degussa in 1942, using a process based on the vapor-phase condensation of formaldehyde and acetaldehyde in absence of oxygen [2]. Later, in 1959, Shell pioneered the production of acrolein through oxidation of propylene over heterogeneous catalysts [3]. Nowadays, the commercial production of acrolein is mostly performed by this method of synthesis, using multicomponent catalysts such as bismuth molybdate-based solids [2] but greener and more sustainable methods have also been developed.

Among these, glycerol dehydration to acrolein has been widely studied during the last decade [6–8]. Most investigations of this process were done over acidic catalysts such as tungstated zirconia and titania, heteropolyacids [9] or zeolites [10,11]. Several catalysts, such as heteropolyacids, were found to exhibit good conversion and selectivity, but with a rapid decrease in activity over time due to severe coking.

* Corresponding author.
E-mail address: aline.auroux@ircelyon.univ-lyon1.fr (A. Auroux).

https://doi.org/10.1016/j.apcata.2020.117871
Received 18 August 2020; Received in revised form 2 October 2020; Accepted 3 October 2020
Available online 06 October 2020
0926-860X/

The use of other catalysts made it possible to maintain catalytic activity for longer times but coking inevitably occurs [12]. As shown by Dalil et al. [13], some coke accumulation is beneficial to acrolein production. During the initial coke formation, the acrolein yield is increasing. However, an excessive coke build up requires frequent regenerations, and various technologies have been investigated to cope with this difficulty [14–18]. The lack of sufficient volumes of glycerine has hindered the development of an industrially competitive process. In Europe, changing regulations on biofuels and multiple count systems on the biofuels derived from "wastes" has reduced the volumes of glycerine produced. In addition, the development of Renewable Diesel (hydrogenated oils and fats) which coproduces propane instead of glycerine has further impacted the glycerine volumes, and therefore the prices.

In parallel to this research, other methods using bio-based products for the production of sustainable acrolein have been developed. Among those alternatives, acrolein production through Oxidative Coupling of Alcohols (OCA) is now considered. This recent process, patented by Dubois et al. [19], is decomposed into two steps. The first step is the simultaneous oxidation of methanol and ethanol to formaldehyde and acetaldehyde respectively over iron-molybdate (FeMoOx) catalyst which already produces some acrolein [20–22]. Then, in order to increase the coupling, it is necessary to boost the cross-aldolization of formaldehyde and acetaldehyde to acrolein over an acid-base catalyst. The final objective would be to produce acrolein in a single reactor, meaning on a single catalyst that would combine a balanced redox and acid-base properties. Such a process would reduce energy consumption, versus the glycerol dehydration route since the reaction is exothermic at a temperature high enough to recover valuable energy, and would still permit the use of renewable resources. It is then necessary to identify the right balance of acid-base properties, in these working conditions (oxidative atmosphere during the aldol coupling).

Several acid-base catalysts have already been used for cross-aldolization of formaldehyde and acetaldehyde, such as zeolites [23–26], mixed oxides [27,28], clays [29], oxides supported on silica [30], hydrotalcites [31], heteropolyacids [31] and magnesium aluminate spinels [32]. These studies have led to different conclusions.

Ai [28,33] concluded that aldol condensation is catalyzed by basic sites, with acrolein production on weak sites while stronger sites promote the production of carbon oxides. Dumitriu et al. [34] proposed that acetaldehyde is activated by basic sites thanks to an H-abstraction on the α-position of carbonyl, making these basic sites necessary for the reaction; acidic sites would be also necessary because they would activate formaldehyde by enhancing electrophilicity of the carbon atom. According to Cobzaru et al. [26], general catalytic activity would be governed by basic properties, even if both acidic and basic sites allow for aldolization. More recently, Lilic et al. [30,31] demonstrated that excessive basicity is detrimental to acrolein production and underlined the necessity for catalysts to have both acidic and basic properties in order to achieve optimal acrolein production. A recent study using magnesium aluminate spinel catalysts confirmed the results obtained by Lilic et al. [32]. Besides, calorimetric investigations led to the formulation of a hypothesis to explain the absence of crotonaldehyde as a side product, namely that the isolation of acetaldehyde molecules at the catalyst surface prevented self-aldolization therefore promoting the cross-aldolization [32].

In this work, the goal is to determine the acid-base properties of spinel catalysts where magnesium was partly or totally substituted by metals such as zinc, copper, cobalt, iron or manganese. These spinels, known to be amphoteric, could constitute good catalysts for this reaction. Besides, substitution of Mg by transition metals appears to be an interesting way to affect the acid-base balance and therefore to increase acrolein yields. The catalytic reaction was performed in gas phase in two separate fixed bed reactors. A redox catalyst (FeMoOx) was used for the oxidation reaction, while the materials under study were tested as acid-base catalysts for the aldolization reaction. Moreover, in the objective of performing the global reaction with a single catalyst, the redox properties of the substitution metals could bring the required bifunctional redox and acid-base character.

The acid-base and adsorptive properties of these catalysts were investigated by adsorption microcalorimetry using NH_3, SO_2, formaldehyde, acetaldehyde and propionaldehyde (used as a substitute for acrolein) vapors as probe molecules. The adsorption microcalorimetry technique allows the simultaneous determination of the number, strength, and strength distribution of the active sites. Besides, Fourier Transform Infrared (FT-IR) spectroscopy was used in order to investigate the mechanisms of adsorption of the reactants. Other physicochemical properties were determined using XRD, chemical analyses, and N_2-adsorption at $-196\,^{\circ}C$.

2. Experimental

2.1. Catalyst characterization

Spinel catalysts, available upon request, synthesized by alum process (using sulfate precursors), with magnesium partly or totally substituted by metals were all graciously provided by Baikowski (Poisy, France). All chemicals were analytical grades purchased from Sigma-Aldrich. Specific surface areas (S_{BET}) were determined by N_2-adsorption at $-196\,^{\circ}C$ with a Micromeritics Flowsorb III apparatus. Prior to nitrogen adsorption, the spinels were pre-treated for 30min at $300\,^{\circ}C$ under nitrogen flow.

The acid-base properties of the spinel catalysts were determined by adsorption microcalorimetry using SO_2 and NH_3 as probe molecules. The experiments were performed at $150\,^{\circ}C$ in a Tian-Calvet heat flow calorimeter (C80 from Setaram) linked to a conventional volumetric apparatus equipped with a Barocel capacitance manometer for pressure measurements, enabling the determination of adsorbed amounts and equilibrium pressure. Prior to the adsorption of small successive doses of probe molecules, each sample was pretreated in a quartz cell overnight at $400\,^{\circ}C$ under vacuum (10^{-5} Pa). Details of the technique and experimental conditions are available elsewhere [35,36]. Reactant adsorption was also studied by adsorption microcalorimetry at $30\,^{\circ}C$ using formaldehyde, acetaldehyde and propionaldehyde as probe molecules.

XRD patterns were recorded on a Bruker D8 Advance A25 diffractometer at room temperature using CuK_{α} radiation (0.154 nm) from 4 to 80° in 0.02° steps with 0.5 s per step.

Chemical analyses were performed using inductively coupled plasma optical emission spectroscopy (ICP-OES) with an ACTIVA spectrometer from Horiba JOBIN YVON. Prior to analysis, the samples were dissolved in a mixture of inorganic acids (H_2SO_4 + HNO_3) and heated to $250-300\,^{\circ}C$.

2.2. FTIR studies

The powders were pressed into self-supporting discs of about 20 mg, placed in a cell with CaF_2 windows and activated under vacuum at $400\,^{\circ}C$. The IR spectra were recorded by a Thermo Scientific Nicolet 8700 Fourier transform spectrometer equipped with a DTGS detector and using OMNIC software. Formaldehyde was obtained by evaporation under vacuum of solid paraformaldehyde (Sigma-Aldrich, 95 % purity). Acetaldehyde (Sigma Aldrich 99.5 % purity) and propionaldehyde (Sigma Aldrich 99.5 % purity) were put through several freeze-pump thaw cycles each day before use. Table S1 displays the major bands obtained for gas-phase formaldehyde, acetaldehyde and propionaldehyde.

2.3. Catalytic test

Two consecutive stainless-steel continuous-flow reactors (R1 and R2) were used to produce acrolein. Simultaneous oxidation of sustainable methanol and ethanol (from Bio-MCN) was carried out in the first

reactor (R1) filled with commercial FeMoOx catalyst (3 g) diluted with steatite (20 g) for temperature control, to produce formaldehyde and acetaldehyde (Reaction 1). At the outlet of the first reactor, the products were directed to the second reactor (R2) filled with spinel-type catalysts (20 g) in order to perform cross-aldolization of formaldehyde and acetaldehyde followed by dehydration to produce acrolein (Reaction 2). The pressure inside the reactors was close to atmospheric pressure. The reactors were heated independently by two salt baths and the reaction temperature was monitored by moving a thermocouple inserted in a thermometric well to identify hot spots in the catalytic bed.

$$CH_3CH_2OH + CH_3OH + O_2 \rightarrow CH_3CHO + HCHO + 2H_2O \quad (1)$$

$$CH_3CHO + HCHO \rightarrow CH_2(OH)CH_2CHO \rightarrow CH_2=CH-CHO + H_2O \quad (2)$$

The chosen conditions for the first reactor were MeOH/EtOH/O_2/N_2 molar ratio = 4:2:8:86, T_1 = 266 °C (salt bath temperature), GHSV = 10 000 or 5000 h^{-1}. Such values were already selected in previous studies in order to get a partial conversion, to be able to detect variations and compare our results with existing literature [32]. The outlet stream for R1 was regularly checked to confirm that activity did not vary over time. GHSV is calculated as the gas flow-rate in normal conditions divided by the estimated volume of the undiluted catalyst. In the second reactor, the temperature (T_2) varied between 266 and 285 °C (salt bath temperature).

The catalysts were compared at conversions lower than 100 %, also with the idea to simulate conditions that would occur in a single reactor where all reagents and products co-exist. The products exiting the second reactor were collected in two sequential traps (cooled to 0 °C using an ice bath). Uncondensable products (O_2, N_2, CO, CO_2) were quantified online, thanks to a micro-GC using a thermal conductivity detector (TCD), with a silica Porous Layer Open Tubular (PLOT) column to measure CO_2 concentration and a molecular sieves column to analyze O_2, N_2 and CO. Condensable products (acrolein, acetaldehyde, methanol, ethanol, crotonaldehyde, and others) were quantified offline by GC with ZB-WAX Plus column (length = 60 m, ID = 0.53 mm, df = 1 µm. Ramp temperature = 8 °C min^{-1} from 40 to 220 °C and then 13 min at 220 °C) equipped with a flame ionization detector (FID). An example of a chromatogram is given in Fig. S1 (Sample (0.8 Mg ; 0.2 Mn) Al_2O_4)

Prior to analysis, formaldehyde was derivatized in a solution of dinitrophenylhydrazine (DNPH) and then quantified offline by GC with HP-5 column (length = 30 m, ID = 0.25 mm, df = 1 µm. Ramp temperature = 15 °C min^{-1} from 60 to 195 °C then 5 °C min^{-1} until 235 °C and then 30 °C min^{-1} until 300 °C) equipped with a flame ionization detector.

The methodology used to determine the conversion (C) of the reactants (methanol, ethanol, formaldehyde and acetaldehyde) and of carbon [%], molar and carbon Yields (Y) of acrolein, acetaldehyde and formaldehyde [%], and selectivity (S) towards acrolein [%] has been described in detail in previous studies [30,32].

3. Results and discussion

3.1. Chemical analysis

Table 1 displays the studied catalysts with their specific surface areas (S_{BET}), sulfur contents and results of chemical analysis (in atomic % and weight%). Table S2 displays the same results with chemical analysis in molarity. The specific surface areas are heterogeneous, varying from 9 $m^2.g^{-1}$ for $ZnAl_2O_4$ to 38 $m^2.g^{-1}$ for (0.8 Mg ; 0.2 Mn) Al_2O_4 and (0.8 Mg ; 0.2Fe) Al_2O_4, while most samples are close to 30 $m^2.g^{-1}$. The chemical analysis results were relatively close to the theoretical contents. Despite the samples were synthesized from sulfate precursors and calcined at high temperature, the sulfur content remains low except for zinc substituted spinels.

Table S2 shows that the spinels with manganese addition contain lower amounts of manganese than expected. Similarly, the metal contents of the other modified spinels always ended up being lower-than expected. Besides, a small deficiency in magnesium is observed for all catalysts. The substitution cationic (+II) metals display varying redox properties. Copper possesses a stronger oxidizing character than zinc and manganese, while cobalt and iron are in between copper and zinc. These redox properties are certainly playing a role in the catalytic activity, together with the acid-base characteristics.

3.2. X-Ray diffraction analysis

Fig. S2 displays the XRD patterns of magnesium aluminate spinel where magnesium was partly or totally substituted by five different metals, namely iron, copper, zinc, manganese and cobalt. 8 peaks centered at 2θ = 19, 31, 36, 45, 55, 59, 65 and 78° can be observed. All these peaks can be attributed to the spinel structure. Contrary to some other spinel catalysts previously studied [32], no phase corresponding to α-alumina was observed in these five samples. However, amorphous phases of metal oxides cannot be excluded.

Fig. S3 displays overlapping peaks near 37° for (0.8 Mg ; 0.2 M) Al_2O_4 (A) and (0.5 Mg ; 0.5 M) Al_2O_4 (B) (where M = Mn, Zn, Co, Cu or Fe). It can be observed that the peaks of the manganese containing samples are shifted towards lower angles compared to other elements, thus underlining the higher ionic radius of divalent manganese compared to the other metals.

From XRD results, lattice parameters, cell volumes and maximum ionic radii in tetrahedral and octahedral sites have been calculated (Table S3). It can be observed that spinels containing manganese displayed higher lattice volumes than other samples. This increased volume, due to the presence of bigger element in the lattice, confirms the observation of shifted XRD peaks to lower angles and thus the higher radius of manganese ions.

Besides, the calculated maximum radius in tetrahedral site (0.64 Å) is lower than the ionic radius for Mn^{2+} in tetrahedral coordination calculated by Shannon [37] (0.66 Å). Therefore, it can be considered that substitution of magnesium by manganese in tetrahedral site generates distortions in the lattice. The hypothesis that manganese ions could have moved from tetrahedral to octahedral sites is plausible for such a big cation. Moreover, an oxidative transfer of Mn from tetrahedral to octahedral sites has already been observed [38,39].

3.3. Acid-base and adsorptive properties of the catalysts

The number, the strength and the strength distribution of active sites have been determined thanks to adsorption microcalorimetry of probe molecules in gas phase coupled to a volumetric line. Ammonia (NH_3), a Lewis and Brønsted base, was used to probe the acidity, and sulfur dioxide (SO_2) was used to titrate basic sites. The experiments were performed at 150 °C on samples pretreated at 400 °C overnight. The resulting differential heats of adsorption of ammonia and SO_2 are displayed versus the adsorbed amount of probe molecule in Fig. 1 The corresponding adsorption isotherms are available in Fig. S4.

Heterogeneous acidity can be seen for all the catalysts. Samples (0.5 Mg ; 0.5 Mn) Al_2O_4 and (0.8 Mg ; 0.2 Mn) Al_2O_4 display the strongest acidity, with initial heats higher than 150 kJ.mol^{-1}. The other catalysts display initial heats between 100 and 150 kJ.mol^{-1}. (0.5 Mg ; 0.5Co) Al_2O_4 shows the highest total adsorbed amount of ammonia, followed by (0.8 Mg ; 0.2Fe) Al_2O_4 and (0.8 Mg ; 0.2 Mn) Al_2O_4. At the opposite, $ZnAl_2O_4$ displays very weak acidic sites with a very low adsorbed amount, which is logical considering the very low specific surface area.

As to basicity, three catalysts displays initial heats higher than 200 kJ.mol^{-1}, and a small plateau can be seen in the 160–180 kJ.mol^{-1} range, indicating the presence of a population of strong basic sites. The

Table 1
List of studied catalysts with surface area, sulfur content and chemical analysis (C.A.).

Catalyst	S_{BET} ($m^2.g^{-1}$)	S (ppm)	CA (at% - wt%)						
			Mg	Al	Zn	Cu	Co	Fe	Mn
(0.8 Mg ; 0.2Fe) Al_2O_4	38	350	10.4 – 12.1	27.2 – 35.1				2.7 –7.2	
(0.8 Mg ; 0.2Cu) Al_2O_4	19	151	10.8 – 12.3	28.5 – 36.1		2.7 – 8.1			
(0.5Co ; 0.5 Mg) Al_2O_4	34	569	6.7 – 7.2	27.9 – 33.5			6.7 – 17.5		
$CoAl_2O_4$	27	549	< 0.1	28.4 – 30.7			13.6 – 32.1		
(0.8 Mg ; 0.2Zn) Al_2O_4	32	1445	10.8 – 12.4	28.0 – 35.8	2.3 – 7.0				
(0.5 Mg ; 0.5Zn) Al_2O_4	29	5251	6.8 – 7.2	28.6 – 33.6	6.6 – 18.8				
$ZnAl_2O_4$	9	7170	< 0.1	28.4 – 30.0	13.1 – 33.4				
(0.8 Mg ; 0.2 Mn) Al_2O_4	38	453	10.7 – 12.4	27.7 – 35.8					2.5 – 6.5
(0.5 Mg ; 0.5 Mn) Al_2O_4	32	285	6.6 – 7.3	27.5 – 33.8					6.1 – 15.3

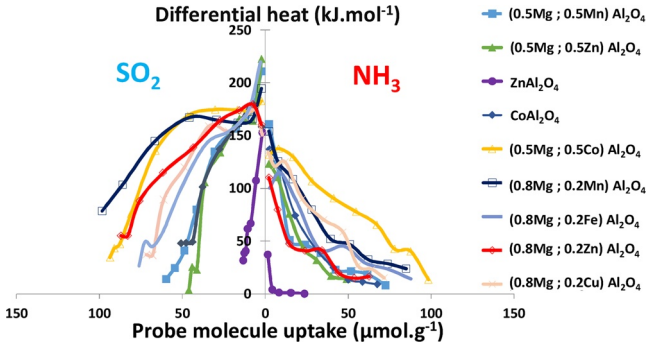

Fig. 1. Differential heats of adsorption of SO_2 (left) and NH_3 (right) for studied spinel catalysts at 150 °C.

highest adsorbed amount of basic sites is shown by (0.8 Mg ; 0.2 Mn) Al_2O_4 and the lowest by $ZnAl_2O_4$. (0.5 Mg ; 0.5Zn) Al_2O_4 and $ZnAl_2O_4$, which are exhibiting the lowest amounts of basic sites per surface area (µmol. m^{-2}) are also displaying the higher sulfur contents. This result confirms that sulfur compounds are preferentially adsorbed on basic sites.

At first glance, the results suggest a dominant basic character for the majority of the catalysts. The results are rather similar to those of a previous microcalorimetric study performed on spinel catalysts [32].

As previously mentioned, adsorption microcalorimetry makes it possible to discriminate between physisorbed and chemisorbed amounts of probe molecules. Table 2 gives the total adsorbed amounts and irreversibly adsorbed amounts for each sample, as well as the ratios of total basic to total acidic sites and strong basic to strong acidic sites.

These ratios give an indication of the overall basic or acidic character of each sample. Adsorption microcalorimetry does not give access to the nature of acid-base sites, but based on the high calcination temperature of the samples, Lewis sites were mostly expected. Nonetheless, the FTIR study (paragraph 3.6) has shown that a few Brønsted sites can be detected.

The results from Table 2 and Fig. 1 confirm the amphoteric character of all the studied samples. With initial heats higher than 150 $kJ.mol^{-1}$, (0.5 Mg ; 0.5 Mn) Al_2O_4 and (0.8 Mg ; 0.2 Mn) Al_2O_4 are the only two catalysts to exhibit strong acidic sites. The others all show medium strength acidic sites, except for $ZnAl_2O_4$ which only displays weak acidic sites. Concerning basicity, all the samples display strong basic sites and even very strong ones ($Q > 200\ kJ.mol^{-1}$) for (0.5 Mg ; 0.5 Mn) Al_2O_4, (0.8 Mg ; 0.2Fe) Al_2O_4 and (0.5 Mg ; 0.5Zn) Al_2O_4. Based on the ratios of total basic to acidic sites and the ratios of strong basic to strong acidic sites, it can be concluded that all the samples have amphoteric character but with a dominant basic character. The cobalt and zinc spinels show the most amphoteric character. Moreover, as shown in Fig. 2, an increase in guest metal content and thus a decrease in magnesium oxide content appears to lead to a decrease in the basic character, confirming the idea that the presence of magnesium oxide enhances the basicity of the catalysts.

From the differential heats of adsorption, it is possible to determine the strength distributions which correspond to the number of sites with a given strength. The results are displayed in Fig. S5 for acidity and Fig. S6 for basicity.

It can be observed that the spinels containing zinc show lower amounts of acidic sites than those containing cobalt, even when the specific surface areas are close to each other. As seen from the differential heats of adsorption, the most acidic catalyst is (0.8 Mg; 0.2 Mn)

Table 2
Q_{init}, V_{irrev} and V_{tot} calculated from adsorption isotherms of SO_2 and NH_3 obtained by microcalorimetry measurements at 150 °C.

Sample	NH_3			SO_2			$Base_{tot}/Acid_{tot}$ [d] V_{tot} [b] [µmolSO_2.g^{-1}]/ V_{tot} [µmolNH_3.g^{-1}]	$Base_{chem}/Acid_{chem}$ [e] V_{irrev} [b] [µmolSO_2.g^{-1}]/ V_{irrev} [µmolNH_3.g^{-1}]
	Q_{init} [a] ($kJ.mol^{-1}$)	V_{total} [b] (µmol.g^{-1})	V_{irrev} [c] (µmol.g^{-1})	Q_{init} [a] ($kJ.mol^{-1}$)	V_{total} [b] (µmol.g^{-1})	V_{irrev} [c] (µmol.g^{-1})		
$MgAl_2O_4$ [32]	169	119.0	48.5	182	58.9	45.0	0.5	0.9
(0.8 Mg ; 0.2 Zn) Al_2O_4	110	43.1	12.0	160	83.5	72.8	1.9	6.0
(0.5 Mg ; 0.5 Zn) Al_2O_4	123	37.9	8.8	223	43.0	32.7	1.1	3.7
$ZnAl_2O_4$	37	14.2	3.8	153	12.2	7.1	0.9	1.9
(0.5 Mg ; 0.5 Co) Al_2O_4	132	78.9	25.6	183	88.8	75.9	1.1	3.0
$CoAl_2O_4$	137	50.0	19.6	158	46.8	35.4	0.9	1.8
(0.8 Mg ; 0.2 Fe) Al_2O_4	100	59.2	16.3	220	67.9	54.1	1.1	3.3
(0.8 Mg ; 0.2 Cu) Al_2O_4	134	55.0	25.9	151	70.3	61.4	1.3	2.4
(0.8 Mg ; 0.2 Mn) Al_2O_4	154	64.1	17.5	195	99.7	89.2	1.6	5.1
(0.5 Mg ; 0.5 Mn) Al_2O_4	161	49.7	15.3	211	53.1	42.2	1.1	2.8

[a] Heat evolved from the first SO_2 or NH_3 dose.
[b] Total amount of SO_2 and NH_3 adsorbed under an equilibrium pressure of 27 Pa.
[c] Amount of chemisorbed SO_2 and NH_3 under an equilibrium pressure of 27 Pa.
[d] Ratio of total basic to acidic sites.
[e] Ratio of chemisorption strong basic to acidic sites.

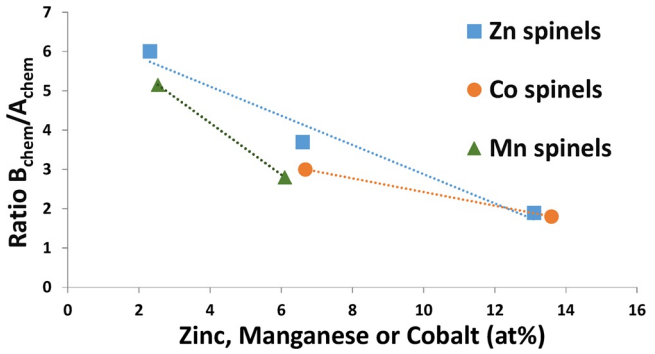

Fig. 2. Ratio of the amounts of strong basic sites to strong acidic sites versus percentage of guest metal atoms.

Al_2O_4 which exhibits strong acidic sites with heats higher than 150 kJ.mol^{-1}. Among the other catalysts, only (0.5 Mg ; 0.5 Mn) Al_2O_4 also displays strong sites (Q > 150 kJ.mol^{-1}).

The same trend is observed for the strength distribution of basic sites, with (0.8 Mg ; 0.2 Mn) Al_2O_4 acting as the most basic catalyst even if other catalysts such as (0.5 Mg ; 0.5 Mn) Al_2O_4 or (0.5 Mg ; 0.5Zn) Al_2O_4 display very strong sites (Q > 200 kJ.mol^{-1}).

In order to study in depth the mechanism of adsorption of reactants at the surface of the catalysts, acetaldehyde and formaldehyde adsorption microcalorimetry investigations have been performed at 30 °C, using the same experimental procedure as those conducted for NH_3 and SO_2. Fig. 3 displays the differential heats of adsorption of acetaldehyde on the left side and formaldehyde on the right side versus amounts of adsorbed probe molecule. The corresponding adsorption isotherms are available in Fig. S7. Experiments with formaldehyde were only performed on a subset of the samples, due to the possibility of oligomerization at this temperature.

As already seen in a previous study performed over unsubstituted magnesium aluminate spinels [32], the acetaldehyde and formaldehyde adsorption curves have similar shapes, leading to the conclusion that the adsorption sites are the same for both molecules. It can also be seen that large amounts of both formaldehyde and acetaldehyde are adsorbed. Concerning acetaldehyde, the presence of a small plateau in the domain of 150 kJ.mol^{-1} can be observed for (0.5 Mg ; 0.5Co) Al_2O_4. This plateau is not seen for the other catalysts. (0.8 Mg ; 0.2Fe) Al_2O_4 shows the largest adsorbed amount, with (0.8 Mg ; 0.2 Mn) Al_2O_4 a close second, while the smallest amount is displayed by $ZnAl_2O_4$. Formaldehyde adsorption seems to follow the same trend. The amount of formaldehyde adsorbed is always higher than that of acetaldehyde. In order to understand this difference of adsorbed amounts, adsorption experiments were also performed at 80 °C for (0.8 Mg ; 0.2 Mn) Al_2O_4 catalyst. The resulting isotherms of adsorption of NH_3, SO_2, acetaldehyde and formaldehyde are displayed in Fig. 4A. Interestingly, at this temperature, the adsorbed amounts of acetaldehyde and

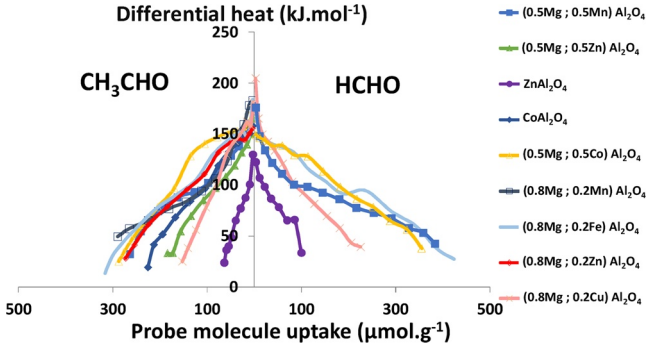

Fig. 3. Differential heats of adsorption of acetaldehyde (left) and formaldehyde (right) for the studied spinel catalysts at 30 °C.

formaldehyde are identical, suggesting a probable oligomerization of formaldehyde at 30 °C. Moreover, the adsorbed amounts of aldehydes are equal to the sum of the NH_3 and SO_2 adsorbed amounts (green and purple isotherms in Fig. 4A). These results evidence the fact that aldehydes are adsorbed both on acidic and basic sites, confirming a previous study performed over spinel catalysts [32].

In order to estimate the adsorption properties of acrolein over spinel catalysts, microcalorimetry experiments have been performed using propionaldehyde as a substitute probe molecule. Fig. 5 displays the differential heats of adsorption of propionaldehyde over the investigated catalysts at 30 °C. The corresponding adsorption isotherms can be seen in Fig. S8.

The differential heats of adsorption of propionaldehyde are very similar to those of acetaldehyde and formaldehyde. Here again, (0.5 Mg ; 0.5Co) Al_2O_4 catalysts is exhibiting a small plateau around 160 kJ.mol^{-1}; and (0.8 Mg ; 0.2Fe) Al_2O_4 and (0.8 Mg ; 0.2 Mn) Al_2O_4 catalysts show the highest total adsorbed amount of propionaldehyde, probably because of their higher specific surface area. As for formaldehyde and acetaldehyde, $ZnAl_2O_4$ displays the lowest heat of adsorption and uptake, with a very small plateau in the domain of weak heats of adsorption (60 kJ.mol^{-1}). Note that $ZnAl_2O_4$ displays the same very small plateau during formaldehyde adsorption.

3.4. Consecutive adsorption of formaldehyde and acetaldehyde

In order to study the competition between adsorption of acetaldehyde and formaldehyde, formaldehyde was first adsorbed on (0.8 Mg ; 0.2 Mn) Al_2O_4 at 80 °C (curve **a** in Fig. 4B). Then, after evacuation, formaldehyde was readsorbed (curve **b**) to determine the physisorbed amount and after a second evacuation, adsorption of acetaldehyde was then performed (curve **c**) at the same temperature. The opposite experiment, adsorption of acetaldehyde (curve **a** in Fig. 4C) followed by readsorption of acetaldehyde (b) and an adsorption of formaldehyde (c), was also performed.

Fig. 4B shows that, after adsorption of formaldehyde and thus saturation of the chemisorption sites, acetaldehyde is not able to adsorb as much as formaldehyde (curves b and c are not superimposed). However, the opposite experiment shows that, after saturation of chemisorption sites by acetaldehyde, formaldehyde is capable to adsorb as much as acetaldehyde (curves b and c in Fig. 4C are superimposed). It is worth noting that multiple processes other than adsorption could possibly occur at the catalyst's surface, such as self-aldolization or oxidation leading to strongly bound formates or acetates which cannot be easily displaced.

Nonetheless, the results suggest that it is not possible to adsorb as much acetaldehyde after formaldehyde chemisorption as formaldehyde after acetaldehyde chemisorption. Therefore, the adsorption sites of the catalyst should have a stronger affinity for formaldehyde than acetaldehyde. Moreover, these results follow the same trend reported in a previous study performed over spinel, where the absence of crotonaldehyde among reaction products was explained by the isolation of acetaldehyde by formaldehyde on the surface of the catalyst, pushing acetaldehyde to react only with formaldehyde to give acrolein [32].

3.5. Catalytic tests

Acrolein is already produced during the first step of reaction over iron molybdate (FeMoOx) catalyst [20,21,30,31], however the yield can be enhanced by using an aldolization reaction to convert acetaldehyde and formaldehyde to acrolein in a second step. To perform this aldolization, acid-base catalysts are necessary. Spinel materials, being amphoteric, were therefore investigated as possible catalysts for the synthesis of acrolein starting from a mixture of alcohols (methanol + ethanol) in the presence of oxygen in a two-step process. The molar ratios of MeOH/EtOH/O_2/N_2 were set at 4/2/8/86 with a GHSV of 10 000 and 5000 h^{-1}. The temperature in Reactor 1 was fixed at

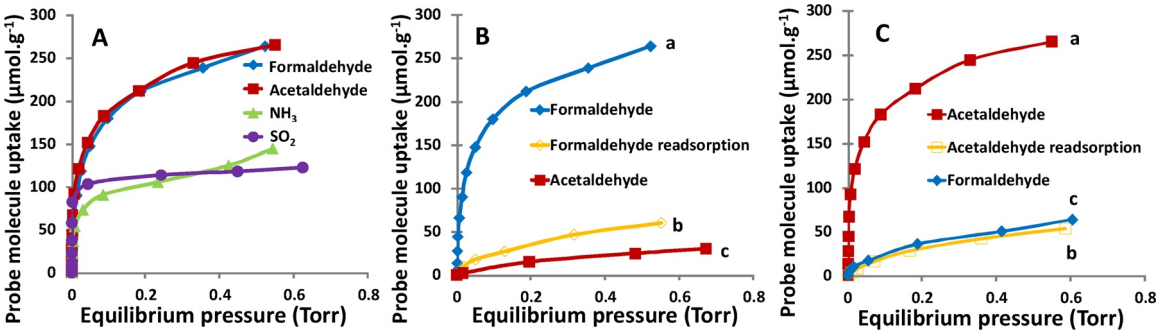

Fig. 4. A: adsorption isotherms of acetaldehyde, formaldehyde, NH_3 and SO_2 for (0.8 Mg ; 0.2 Mn) Al_2O_4 at 80 °C ; B: isotherms of formaldehyde adsorption (a) and readsorption of formaldehyde (b) followed by adsorption of acetaldehyde (c) at 80 °C on (0.8 Mg ; 0.2 Mn) Al_2O_4 ; C: isotherms of acetaldehyde adsorption (a) and readsorption of acetaldehyde (b) followed by adsorption of formaldehyde (c) at 80 °C on (0.8 Mg ; 0.2 Mn) Al_2O_4.

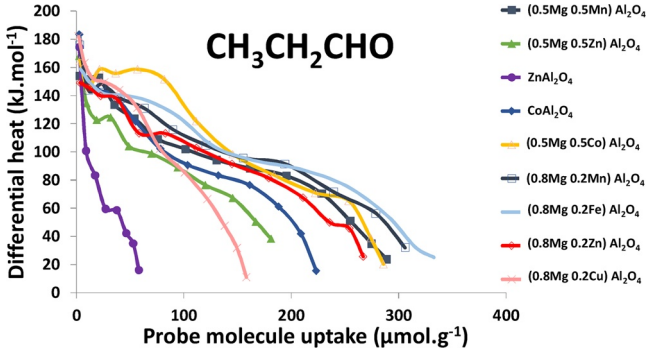

Fig. 5. Differential heats of adsorption of propionaldehyde versus coverage over the studied spinel catalysts at 30 °C.

266 °C. Under these conditions, the mixture of alcohols was not completely converted. For GHSV of 5000 h^{-1}, ethanol conversion reached 90 % while methanol conversion was 69 %. At the outlet of R1, acrolein, acetaldehyde, formaldehyde and COx production reached 13, 21, 13 and 5.5 % respectively with 6 vol% of residual O_2. After the first reactor, the mixture of formaldehyde, acetaldehyde, methanol and ethanol was directly sent into the second reactor to produce acrolein through cross-aldolization. Tests have been performed at 266 and 285 °C. Higher temperatures have not been tested, in order to limit the production of carbon oxides. Carbon balance was always between 75 and 90 %. Table 3 displays the yields of acrolein, (CO + CO_2), acetaldehyde, formaldehyde, and the conversion of methanol and ethanol at the outlet of R2 for zinc, cobalt, manganese, iron and copper based spinel catalysts. Table S4 shows the composition of the gaseous mixture at the outlet of R1.

Among the zinc spinels, the best catalyst appear to be $ZnAl_2O_4$ with 22 % acrolein yield and 7 % COx production followed by (0.5 Mg ; 0.5Zn) Al_2O_4 with 21 % of acrolein and 7 % of COx. Nonetheless, these catalysts are deactivating very quickly. Looking at these results, the quantity of zinc in the sample does not seem to have a significant impact on the acrolein production. Concerning cobalt based catalysts, the scheme is relatively similar; the best results are exhibited by $CoAl_2O_4$ with 19 % acrolein yield. (0.5 Mg ; 0.5Co) Al_2O_4 led to a very high production of carbon oxides, due to a very strong hotspot during the experiment. The acrolein yield is probably underestimated due to this hotspot. In this case again, it is impossible to see a correlation between the quantity of cobalt in the sample and the acrolein production. For copper spinel, an important hotspot was already seen at 215 °C, probably because of the highly oxidative character of copper. Thus, the reaction was performed at 200 °C over this sample, which led to a very weak acrolein yield of 14 %, barely higher than that already achieved after reactor 1 (13 %). Iron spinel displayed an interesting yield of acrolein (26 %) even if the carbon oxides yield is still quite high (19 %). In order to limit over-oxidation to COx, a decrease in the O_2 amount in the feed gas mixture, from 8% to 5%, was attempted. This led to a small decrease in both CO_2 and acrolein yields. An increase of temperature led to COx formation rather than acrolein production. Fig. S9, which shows the COx production *vs* the amount of basic sites ($Q > 50\ kJ.mol^{-1}$), leads to the conclusion that an increased amount of basic sites can result in an elevated production of carbon oxides, thus confirming previous work performed by Lilic et al. [31]. Besides, it appears that not only the basicity but also the nature of substitution metal plays a role. Indeed, for example, COx production is quite low with zinc compared to cobalt, suggesting that both redox and acid-base properties have an influence on the catalytic performance.

The most promising results come from manganese spinels. Indeed, the best result is displayed by (0.8 Mg ; 0.2 Mn) Al_2O_4 with 31 % of acrolein yield at 285 °C with a carbon balance of 87 %. In addition to that, nearly 30 % yield of acrolein was also obtained at 266 °C, making it possible to consider a setup were FeMoOx and spinel catalysts would

Table 3
Catalytic tests results obtained over spinel-based catalysts after reactor 2 at 285 °C.

Sample	Yield (Y) or conversion (C)					
	C_{MeOH} [%]	C_{EtOH} [%]	$Y_{acrolein}$ [%]	$Y_{formaldehyde}$ [%]	$Y_{acetaldehyde}$ [%]	Y_{COx} [%]
$MgAl_2O_4$ [32]	66	96	27	9	15	10
(0.8 Mg ; 0.2Zn) Al_2O_4	67	92	20	13	15	8
(0.5 Mg ; 0.5Zn) Al_2O_4	62	96	21	11	20	7
$ZnAl_2O_4$	70	90	22	12	20	7
(0.5 Mg ; 0.5Co) Al_2O_4	73	96	17	9	15	27
$CoAl_2O_4$	63	94	19	14	20	9
(0.8 Mg ; 0.2 Mn) Al_2O_4	60	97	31	5	11	17
(0.5 Mg ; 0.5 Mn) Al_2O_4	60	95	30	6	9	13
(0.8 Mg ; 0.2Fe) Al_2O_4	67	98	26	8	11	19
(0.8 Mg ; 0.2Cu) Al_2O_4 (at 200 °C)	68	89	14	31	21	10

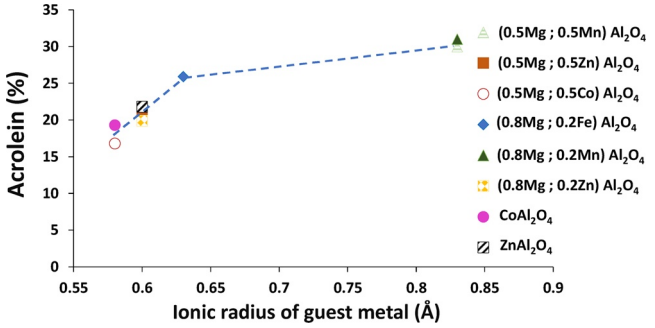

Fig. 6. Acrolein production versus the ionic radius of guest metals.

be placed in the same reactor to produce acrolein. Surprisingly, methanol conversion after reactor 1 (69 %) is nearly always higher than after reactor 2, possibly due to the Cannizzaro disproportionation of formaldehyde leading to formate species and methanol.

Fig. 6 displays the acrolein yield versus the ionic radius of each guest metal in tetrahedral (Fe, Zn and Co) and octahedral sites (Mn). These radii have been taken from Shannon [37,40]. It can be observed that acrolein production clearly depends on the cation species and increases with increasing ionic radius. The different ionic radii probably affect not only the lattice parameters, but also the bond lengths and the electronic density around the cationic centers, inducing differences in catalytic activity. The ionic radius also enters into the calculation of the ionic potential (Z/r) considered by Hu et al. [41] as the polarizing ability of the cation and hence the ability to influence electron density at neighbouring atoms. It might be possible that a high ionic potential (represented by a smaller ionic radius in this case) could have effects on electron movements and bond stretchings, thus preventing some formation of transition states.

Moreover, as previously said, contrary to other elements, Mn(II) could undergo oxidative transfer from a tetrahedral site to Mn(III) in an octahedral site. Jacobs et al. [38] suggested that octahedral sites are exposed almost exclusively at the surface of spinel oxides and that only these sites participate to the reaction. This could explain the better results obtained with manganese compared to other spinel catalysts.

Given the relatively good acrolein yield exhibited by (0.8 Mg ; 0.2 Mn) Al_2O_4 at the temperature of the first reactor (266 °C), the oxidative coupling of alcohols has also been performed in a single reactor. FeMoOx (3 g) and spinel catalysts (20 g) were diluted with steatite (20 g). The conditions were exactly the same as in the two-reactor experiment (MeOH/EtOH/O_2/N_2 molar ratio = 4:2:8:86, T = 266 °C, GHSV = 5000 h^{-1}). This experiment has shown the best results achieved so far for this configuration and this temperature, with 27 % of acrolein (compared to only 13 % exiting from the first reactor) and 14 % of CO + CO_2 production. These results are close to those obtained in the two-step experiment at higher temperature, confirming that it is possible to mix the two catalysts without expecting a decrease in acrolein production.

3.6. FTIR study

In addition to the adsorption microcalorimetry study, an investigation was performed using Fourier Transform Infrared spectroscopy. As in the case of microcalorimetry, formaldehyde, acetaldehyde and propionaldehyde were used as probe molecules. Infrared studies of the adsorption of light aldehydes have already been reported in the literature over materials such as MgO [42–44], Mo/Sn oxides [45], cobalt supported on ZnO [46], silica-supported oxides and metals [47–49], titania [43,50–54], ceria [52], alumina [52,54] but also zeolites [55]. In our case, five magnesium aluminate spinels where magnesium was partially substituted by iron, copper, zinc, cobalt and manganese were used. The spectroscopic analyses were performed on samples in self-supported pellets. After a pretreatment overnight at 400 °C under vacuum, an adsorption was carried out at room temperature (RT) followed by desorptions at RT, 100, 200, 300, and 400 °C. After each step, an infrared spectrum was recorded at room temperature.

3.6.1. Formaldehyde adsorption

Since formaldehyde is a reactant for the cross-aldolization of aldehydes to produce acrolein, its adsorption over spinel catalysts has been studied in order to investigate the mechanism of adsorption at the surface of catalysts. Only few publications have reported on the adsorption of formaldehyde over mixed oxide surfaces. Among these, Busca et al. [42] reported the quick formation of formate species at the surface of magnesium oxide at room temperature. Coordinative formaldehyde has been identified only at low temperatures (around -100 °C) [42]. The formation of formate species has also been reported on alumina and ferrite [56]. Fig. S10 represents the spectra (between 1000 and 3900 cm^{-1}) after adsorption of formaldehyde followed by desorption at 100, 200, 300 and 400 °C on magnesium aluminate spinels where magnesium was partly substituted by manganese which exhibited among the best catalytic results. Fig. 7 displays the same spectra between 1000 and 1900 cm^{-1}. The spectra of magnesium aluminate spinels where magnesium was partly substituted by iron, copper, cobalt, and zinc are available in Figs. S11-S14.

The presence of isolated hydroxyls around 3700 cm^{-1} is easily observed on the pretreated sample. There is also a peak at 1200 cm^{-1} which does not seem to be sensitive to adsorbate and could be assigned to bulk sulfate species in the catalyst [57,58]. The isolated hydroxyls disappear when adsorption is performed, and instead a large band is observed at around 3500 cm^{-1}, characteristic of linked hydroxyls. In addition, after adsorption of formaldehyde new peaks appear between

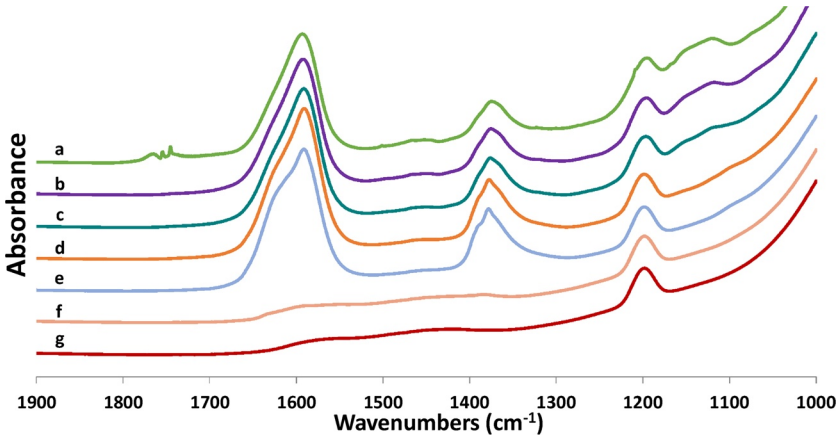

Fig. 7. FTIR spectra (1000-1900 cm^{-1}) of formaldehyde adsorbed on (0.5 Mg ; 0.5 Mn) Al_2O_4 at RT (a) followed by a desorption at RT (b), 100 °C (c), 200 °C (d), 300 °C (e) and 400 °C (f). The pretreated sample curve is in red (g). (For interpretation of the references to colour in this figure legend, the reader is referred to the web version of this article.)

2700 and 3000 cm^{-1} which could be attributed to ν(CH) of formate species [42,56,59]. The more interesting region of the spectra is that between 1000 and 1900 cm^{-1}. In this region, multiple peaks appear after adsorption. The most prominent peak is centered at 1592 cm^{-1}, and accompanied by a smaller peak centered at 1370 cm^{-1}. A small triplet is seen at 1750 cm^{-1}, a large band is observed between 1120 and 1150 cm^{-1} and a very small band at 1070 cm^{-1} can also be seen. The peak at 1750 cm^{-1} is only observed after adsorption, and disappears after the first desorption at room temperature. This is indicative of weakly adsorbed species, and can be attributed to gaseous formaldehyde. The very small band at 1070 cm^{-1} has been attributed in the literature to methoxy groups [42,60]. A similar explanation appears likely for the band centered at 1130 cm^{-1}, which remains visible until desorption at 200 °C, suggesting a relatively strong adsorption. Meanwhile, the two main peaks at 1370 and 1592 cm^{-1} can be attributed to $\nu_{(s)}$ CO_2- and $\nu_{(as)}$ CO_2- of formate species [42,60–62]. It is interesting to notice that these two peaks disappear upon desorption at 400 °C but, for the other studied spinel catalysts (see Figs. S11-S14), these bands are still present at 400 °C. This earlier disappearance could be linked to the better catalytic results of manganese spinels. Nonetheless, these high desorption temperatures indicate very strong adsorption on the surface. The presence of methoxide coupled to formate species could be related to a Cannizzaro disproportionation of formaldehyde as described by Busca et al. [42] and already reported on model magnesia by Peng et al. [63]. It is worth noting that, in our experiments, the conversion of methanol during catalytic test was lower after reactor 2 than after reactor 1, which suggests a "synthesis" of methanol during the catalytic run, consistent with the hypothesis of a Cannizzaro reaction over our spinel catalysts.

3.6.2. Acetaldehyde adsorption

FT-IR spectroscopy has also been used to investigate the mechanism of adsorption of acetaldehyde over the studied spinel catalysts. Fig. S15 displays the spectra of spinel catalyst (0.5 Mg ; 0.5 Mn) Al_2O_4 in the $1000-1900\ cm^{-1}$ region. Spectra of magnesium aluminate spinel where magnesium was partly substituted by iron, copper, cobalt, and zinc are available in Figs. S16-S19.

As in the case of formaldehyde, the isolated hydroxyls evidenced by a band around 3700 cm^{-1} in the spectrum of the pretreated sample disappear after adsorption and give rise to a large band around 3500 cm^{-1} characteristic of linked hydroxyls. An additional triplet can be observed after adsorption between 2700 and 3000 cm^{-1}. This can be assigned to ν(CH) and $\nu(CH_3)$ of acetaldehyde or of a product of reaction of acetaldehyde such as crotonaldehyde. Here again, the most interesting part of spectra is the carboxylate region where multiple peaks can be observed. A peak at 1760 cm^{-1} can be seen on the spectrum after adsorption but not after desorption at room temperature, indicating a weak adsorption. This has been attributed to gaseous acetaldehyde. A more prominent peak is seen at 1710 cm^{-1}, with a shoulder at 1670 cm^{-1} after adsorption and until 300 °C, corresponding to more strongly adsorbed species. Other peaks can be observed at 1580 cm^{-1} with a shoulder at 1600 cm^{-1}, around 1430 cm^{-1}, at 1370 cm^{-1}, 1275 cm^{-1}, and a very small one at 1090 cm^{-1} accompanied by a large band centered at 1150 cm^{-1}. Two isosbestic points (Fig. S20) exist at 1640 and 1415 cm^{-1} suggesting the decomposition or reaction of certain species to form other species as the temperature increases.

It is particularly difficult to distinguish the nature of the different present species, because of the numerous possibilities and the lack of complete agreement among sources in the literature. Some studies notice the presence of acetate species [43,46,61,64–66] by assigning peaks around 1580 and 1430 cm^{-1} to symmetric and asymmetric stretching vibration of COO- deriving from a Cannizzaro like reaction or oxidation. Other authors have concluded that a Cannizzarro reaction seems rather unlikely because it would normally require an aldehyde without available hydrogen in the α-position of the carbonyl group [48]. Those authors prefer to conclude that the aldehyde transforms into surface enolates which could then polymerize or react to produce other aldehydes such as crotonaldehyde [47,48,52,54,67]. In this case, the peak at 1712 cm^{-1} could be assigned to carbonyl groups of acetaldehyde adsorbed on one of the metals. The band at 1670 cm^{-1} could be attributed to carbonyl groups of a reaction product of acetaldehyde such as crotonaldehyde for example, while the peak at 1580 cm^{-1} and its shoulder at 1600 cm^{-1} would be due to presence of either enolate or crotonaldehyde. It is worth noting that these two peaks, and particularly the peak at 1600 cm^{-1}, increase in intensity until 400 °C. This could indicate the presence of two different species arising from the transformation of acetaldehyde or a reaction product. The peak at 1450 cm^{-1} could be attributed to $\delta(CH_3)$ of acetaldehyde and/or crotonaldehyde, while the band at 1380 cm^{-1} seems to be linked with the peak at 1710 cm^{-1} and thus may be assigned to ρw(CHO) of acetaldehyde. Nonetheless, the presence of residual adsorbed aldehyde at the surface of the oxide at 400 °C is not certain; besides, a slight shift can be detected for the peak at 1450 cm^{-1}. A reaction could possibly happen at this temperature, such as the formation of acetate arising from over-oxidation of aldehyde products. Acetate species has previously been observed at high temperature after aldehyde adsorption on alumina, as reported by Raskó et al. [52]. Of course, it is also impossible to exclude the presence of carbonates arising from reaction on the surface of catalysts. Some species are still present at 400 °C, which is 115 °C more than the catalytic test temperature. This presence of non-desorbed species on the surface, coupled to a possible disproportionation of formaldehyde, could hypothetically explain the relatively low yield of acrolein achieved by our catalysts.

3.6.3. Propionaldehyde adsorption

FTIR spectroscopy has also been used to study the adsorption of propionaldehyde, used as a substitute for acrolein, over (0.5 Mg ; 0.5 Mn) Al_2O_4. Fig. S21 shows the FTIR spectra of the (0.5 Mg ; 0.5 Mn) Al_2O_4 catalyst after propionaldehyde adsorption followed by desorption at 100, 200, 300 and 400 °C. Spectra of magnesium aluminate spinel where magnesium was partially substituted by iron, copper, cobalt, and zinc are available in Figs. S22-S25. The adsorption of propionaldehyde has been studied less extensively than that of acetaldehyde, but some adsorption studies over oxides exist in the literature [44,54,68].

As in the case of acetaldehyde, there are multiple peaks in the carboxylate region. Here again, after adsorption it is possible to see band at 1760 cm^{-1} which disappear after desorption at room temperature. A second peak at 1740 cm^{-1} can be seen until 100 °C. A third band around 1700 cm^{-1} is visible after adsorption and then seems to increase in intensity after desorption at 100 °C and disappear between 200 and 300 °C. Other peaks are visible at 1560 cm^{-1}, 1460 with a shoulder at 1455 cm^{-1}, 1420, 1380 and 1300 cm^{-1}. The spectra are relatively close to those of acetaldehyde adsorption. The bands at 1760 cm^{-1} and 1740 cm^{-1} can be attributed to gaseous and physisorbed propionaldehyde. The peak at 1700 cm^{-1} seems to shift to 1680 cm^{-1} from adsorption to desorption at 200 °C. Relying on the literature and following the attribution made for acetaldehyde adsorption, it could be ascribed to an aldol product [55]. The peak at 1560 cm^{-1} could be assigned to C=C of unsaturated aldehyde, while the band at 1470 cm^{-1} is tentatively assigned to deformation of methyl groups. Meanwhile, the peak at 1380 cm^{-1} probably corresponds to symmetric deformation of methyl groups in carbonyl compounds such as propionates [69], propionaldehyde or propionaldehyde reaction products [54].

After increasing the desorption temperature, a band at 1590 cm^{-1} appears. By comparing with the acetaldehyde spectra, it is possible that propionaldehyde undergoes aldolization, polymerization, or even over-oxidation to form propionate species [61,69].

Here again, the presence of bands at 400 °C indicates the existence of strongly adsorbed species. The presence of multiple different species is also an indication of the likely reactive character of acrolein over the studied materials. This suggests that the produced acrolein may over-

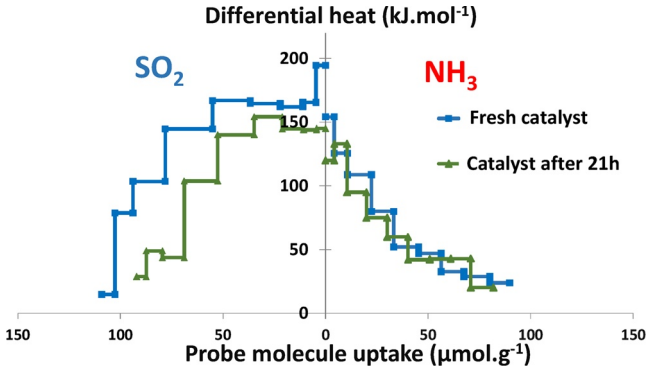

Fig. 8. Differential heats of adsorption of NH_3 (right) and SO_2 (left) at 150 °C for (0.8 Mg ; 0.2 Mn) Al_2O_4: fresh catalyst (blue) and after 21 h (green). (For interpretation of the references to colour in this figure legend, the reader is referred to the web version of this article.)

react at the surface of the catalysts, which might explain the reduced yield of acrolein observed at the outlet of reactor 2.

3.7. Characterization of the used catalysts

Fig. 8 represents the differential heats of adsorption of NH_3 (right) and SO_2 (left) for fresh (0.8 Mg ; 0.2 Mn) Al_2O_4 (blue) and (0.8 Mg ; 0.2 Mn) Al_2O_4 after 21 h of catalytic testing (green). After 21 h, acidity does not seem to be affected. Concerning the basicity, the decrease in number and strength of sites is a little more marked than for acidity. Basic sites are still present in important amounts, even if the strongest basic sites ($Q_{diff} > 150$ kJ.mol^{-1}) disappeared during the reaction. Nonetheless, the yields of acrolein after 21 h remained stable (Fig. S26). This suggests that coke deposition seems to preferentially poison the basic sites, which is logical considering the acidic character of CO_2, but acrolein production is able to continue and remain stable thanks to the presence of medium basic and acidic sites; this is in agreement with the results of previous study [30].This study confirms that coke passivates some selective sites and is not detrimental to the acrolein selectivity [13].

4. Conclusion

Adsorption microcalorimetry of NH_3 and SO_2 probes has been used to determine the acid-base properties of various magnesium aluminate spinels where magnesium was partly or totally substituted by metals such as iron, cobalt, manganese, copper and zinc. Microcalorimetry has also been used to determine the adsorptive properties of reactants (formaldehyde, acetaldehyde, propionaldehyde) for the production of acrolein by cross-aldolization by using them as molecular probes. In addition to microcalorimetry, FTIR spectroscopy has been used to provide further insights into the mechanism of adsorption. These adsorptive properties have been correlated to the results of a catalytic study of acrolein production in oxidizing conditions over these materials.

Among all the studied catalysts, the best production of acrolein was achieved by the magnesium aluminate spinel where magnesium was partly or totally substituted by manganese. Contrary to a previous study performed over xMgO yAl_2O_4 spinels [32], the microcalorimetric study has shown that the acidic and basic properties do not seem to be the key factors explaining this higher activity for manganese spinel. The redox character of the substitution metal plays certainly also a role. Moreover, this study has shown that an increase in cation radius of the guest metal seems to have a positive influence on the acrolein production, possibly thanks to the modification of the lattice parameter, bond length and electronic properties around the cationic centers. The spectroscopic study has made it possible to better understand the transformations undergone by aldehydes at the surface of the catalysts. Formate species were detected upon formaldehyde adsorption at room temperature, indicating a possible Cannizzaro disproportionation, while the investigation of acetaldehyde adsorption suggested that some reaction such as polymerization, oxidation or aldolisation to higher products occurred, possibly explaining the relatively low acrolein yields obtained during catalytic investigations.

Oxidative coupling of alcohols is a promising alternative pathway to produce acrolein from biosourced materials. The catalytic materials devised so far still exhibit relatively low yields, and further investigations of factors such as the influence of the gas mixture composition or the influence of water presence during the reaction will be necessary in order to enhance those yields. Nonetheless, this study makes it possible to better comprehend the adsorption mechanisms occurring on the surface and their implications; this is a helpful step towards the design of more effective catalysts by tuning the surface properties of these solids.

CRediT authorship contribution statement

Vincent Folliard: Investigation, Formal analysis, Writing - original draft. **Georgeta Postole:** Supervision, Writing - review & editing. **Livia Marra:** Investigation. **Jean-Luc Dubois:** Conceptualization, Supervision, Writing - review & editing. **Aline Auroux:** Conceptualization, Supervision, Project administration, Writing - review & editing.

Declaration of Competing Interest

The authors declare that they have no known competing financial interests or personal relationships that could have appeared to influence the work reported in this paper.

Acknowledgements

The authors acknowledge the scientific services of IRCELYON, as well as Corentin Faravel and Zineb Gouighri for their valuable experimental work and Françoise Bosselet for XRD measurements. Dr. Philippe Auroy from Baikowski and Dr. Jean-François Devaux from Arkema are also acknowledged for spinel catalysts supply and fruitful discussions.

Appendix A. Supplementary data

Supplementary material related to this article can be found, in the online version, at doi:https://doi.org/10.1016/j.apcata.2020.117871.

References

[1] Intergovernmental Panel on Climate Change, Global Warming of 1.5°C, (2018).
[2] D. Arntz, A. Fischer, M. Höpp, S. Jacobi, J. Sauer, T. Ohara, T. Sato, N. Shimizu, H. Schwind, in Wiley-VCH Verlag GmbH & Co. KGaA (Ed.), Ullmann's Encyclopedia of Industrial Chemistry, Wiley-VCH Verlag GmbH & Co. KGaA, Weinheim, Germany, 2007, https://doi.org/10.1002/14356007.a01_149.pub2.
[3] L. Liu, X.P. Ye, J.J. Bozell, ChemSusChem 5 (2012) 1162–1180, https://doi.org/10.1002/cssc.201100447.
[4] R.K. Grasselli, F. Trifirò, Rend. Lincei 28 (2017) 59–67, https://doi.org/10.1007/s12210-017-0610-6.
[5] R. Beerthuis, G. Rothenberg, N.R. Shiju, Green Chem. 17 (2015) 1341–1361, https://doi.org/10.1039/C4GC02076F.
[6] B. Katryniok, S. Paul, M. Capron, F. Dumeignil, ChemSusChem 2 (2009) 719–730, https://doi.org/10.1002/cssc.200900134.
[7] B. Katryniok, S. Paul, V. Bellière-Baca, P. Rey, F. Dumeignil, Green Chem. 12 (2010) 2079, https://doi.org/10.1039/c0gc00307g.
[8] B. Katryniok, S. Paul, F. Dumeignil, ACS Catal. 3 (2013) 1819–1834, https://doi.org/10.1021/cs400354p.
[9] E. Tsukuda, S. Sato, R. Takahashi, T. Sodesawa, Catal. Commun. 8 (2007) 1349–1353, https://doi.org/10.1016/j.catcom.2006.12.006.
[10] J. Shan, Z. Li, S. Zhu, H. Liu, J. Li, J. Wang, W. Fan, Catalysts 9 (2019) 121, https://doi.org/10.3390/catal9020121.

[11] X. Ren, F. Zhang, M. Sudhakar, N. Wang, J. Dai, L. Liu, Catal. Today 332 (2019) 20–27, https://doi.org/10.1016/j.cattod.2018.08.012.
[12] P. Lauriol-Garbey, G. Postole, S. Loridant, A. Auroux, V. Belliere-Baca, P. Rey, J.M.M. Millet, Appl. Catal. B 106 (2011) 94–102, https://doi.org/10.1016/j.apcatb.2011.05.011 S0926337311002128.
[13] M. Dalil, M. Edake, C. Sudeau, J.-L. Dubois, G.S. Patience, Appl. Catal. A Gen. 522 (2016) 80–89, https://doi.org/10.1016/j.apcata.2016.04.022.
[14] J.-L. Dubois, G. Patience, US530697B2, 2013.
[15] J.-L. Dubois, G. Patience, US9427718B2, 2016.
[16] J.-L. Dubois, C. Duquenne, W. Holderich, US7396962B1, 2011.
[17] J.-L. Dubois, US9259707B2, 2016.
[18] B.R. Sereshki, S.-J. Balan, G.S. Patience, J.-L. Dubois, Ind. Eng. Chem. Res. 49 (2010) 1050–1056, https://doi.org/10.1021/ie9006968.
[19] J.L. Dubois, M. Capron, F. Dumeignil, US9365478B2, 2016.
[20] A. Borowiec, J.F. Devaux, J.L. Dubois, L. Jouenne, M. Bigan, P. Simon, M. Trentesaux, J. Faye, M. Capron, F. Dumeignil, Green Chem. 19 (2017) 2666–2674, https://doi.org/10.1039/C7GC00341B.
[21] A. Borowiec, A. Lilić, J.-C. Morin, J.-F. Devaux, J.-L. Dubois, S. Bennici, A. Auroux, M. Capron, F. Dumeignil, Appl. Catal. B 237 (2018) 149–157, https://doi.org/10.1016/j.apcatb.2018.05.076.
[22] P.G. Pries De Oliveira, J.G. Eon, C. Moraes, L. Gorenstin Appel, Informativo Do INT 17 (1985) 25–30.
[23] E. Dumitriu, N. Bilba, M. Lupascu, A. Azzouz, V. Hulea, G. Cirje, D. Nibou, J. Catal. 147 (1994) 133–139, https://doi.org/10.1006/jcat.1994.1123.
[24] E. Dumitriu, V. Hulea, I. Fechete, A. Auroux, J.-F. Lacaze, C. Guimon, Microporous Mesoporous Mater. 43 (2001) 341–359, https://doi.org/10.1016/S1387-1811(01)00265-7.
[25] E. Dumitriu, V. Hulea, N. Bilba, G. Carja, A. Azzouz, J. Mol. Catal. 79 (1993) 175–185, https://doi.org/10.1016/0304-5102(93)85100-8.
[26] C. Cobzaru, S. Oprea, E. Dumitriu, V. Hulea, A. Applied Catalysis, General 351 (2008) 253–258, https://doi.org/10.1016/j.apcata.2008.09.024.
[27] W.J. Palion, S. Malinowski, React. Kinet. Catal. Lett. 1 (1974) 461–465, https://doi.org/10.1007/BF02074480.
[28] M. Ai, Bull. Chem. Soc. Jpn. 64 (1991) 1341–1345, https://doi.org/10.1246/bcsj.64.1342.
[29] A. Azzouz, D. Messad, D. Nistor, C. Catrinescu, A. Zvolinschi, S. Asaftei, Appl. Catal. A Gen. 241 (2003) 1–13, https://doi.org/10.1016/S0926-860X(02)00524-0.
[30] A. Lilić, S. Bennici, J.-F. Devaux, J.-L. Dubois, A. Auroux, ChemSusChem 10 (2017) 1916–1930, https://doi.org/10.1002/cssc.201700230.
[31] A. Lilić, T. Wei, S. Bennici, J.-F. Devaux, J.-L. Dubois, A. Auroux, ChemSusChem 10 (2017) 3459–3472, https://doi.org/10.1002/cssc.201701040.
[32] V. Folliard, G. Postole, J.-F. Devaux, J.-L. Dubois, L. Marra, A. Auroux, Appl. Catal. B (2019), https://doi.org/10.1016/j.apcatb.2019.118421.
[33] M. Ai, Bull. Chem. Soc. Jpn. 64 (1991) 1346–1350, https://doi.org/10.1246/bcsj.64.1346.
[34] E. Dumitriu, V. Hulea, C. Chelaru, C. Catrinescu, D. Tichit, R. Durand, Appl. Catal. A Gen. 178 (1999) 145–157, https://doi.org/10.1016/S0926-860X(98)00282-8.
[35] A. Auroux, Calorimetry and Thermal Methods in Catalysis, Springer, New York, 2013, https://doi.org/10.1007/978-3-642-11954-5.
[36] A. Auroux, A. Gervasini, J. Phys. Chem. 94 (1990) 6371–6379, https://doi.org/10.1021/j100379a041.
[37] R.D. Shannon, Acta Crystallographica Section A. 32 (1976) 751–767, https://doi.org/10.1107/S0567739476001551.
[38] J.P. Jacobs, A. Maltha, J.G.H. Reintjes, J. Drimal, V. Ponec, H.H. Brongersma, J. Catal. 147 (1994) 294–300, https://doi.org/10.1006/jcat.1994.1140.
[39] A. Maltha, H.F. Kist, B. Brunet, J. Ziolkowski, H. Onishi, Y. Iwasawa, V. Ponec, J. Catal. 149 (1994) 356–363, https://doi.org/10.1006/jcat.1994.1303.
[40] H.St.C. O'Neill, A. Navrotsky, Am. Mineral. 68 (1983) 181–194.
[41] J. Hu, R.C. Burns, J. Catal. 195 (2000) 360–375, https://doi.org/10.1006/jcat.2000.2987.
[42] G. Busca, J. Lamotte, J.C. Lavalley, V. Lorenzelli, J. Am. Chem. Soc. 109 (1987) 5197–5202, https://doi.org/10.1021/ja00251a025.
[43] Z.D. Young, S. Hanspal, R.J. Davis, ACS Catal. 6 (2016) 3193–3202, https://doi.org/10.1021/acscatal.6b00264.
[44] K. Akutu, H. Kabashima, T. Seki, H. Hattori, Appl. Catal. A Gen. 247 (2003) 65–74, https://doi.org/10.1016/S0926-860X(03)00124-8.
[45] V. Lochař, Appl. Catal. A Gen. 309 (2006) 33–36, https://doi.org/10.1016/j.apcata.2006.04.030.
[46] J.M. Guil, N. Homs, J. Llorca, P. Ramírez de la Piscina, J. Phys. Chem. B 109 (2005) 10813–10819, https://doi.org/10.1021/jp050414k.
[47] V.V. Ordomsky, V.L. Sushkevich, I.I. Ivanova, J. Mol. Catal. A Chem. 333 (2010) 85–93, https://doi.org/10.1016/j.molcata.2010.10.001.
[48] W.E. Taifan, G.X. Yan, J. Baltrusaitis, Catal. Sci. Technol. 7 (2017) 4648–4668, https://doi.org/10.1039/C7CY01556A.
[49] G.J. Millar, C.H. Rochester, K.C. Waugh, J. Chem. Soc. Faraday Trans. 87 (1991) 2785–2793, https://doi.org/10.1039/FT9918702785.
[50] J.E. Rekoske, M.A. Barteau, Ind. Eng. Chem. Res. 50 (2011) 41–51, https://doi.org/10.1021/ie100394v.
[51] J. Raskó, T. Kecskés, J. Kiss, Appl. Catal. A Gen. 287 (2005) 244–251, https://doi.org/10.1016/j.apcata.2005.04.004.
[52] J. Raskó, J. Kiss, Appl. Catal. A Gen. 287 (2005) 252–260, https://doi.org/10.1016/j.apcata.2005.04.003.
[53] M. Singh, N. Zhou, D.K. Paul, K.J. Klabunde, J. Catal. 260 (2008) 371–379, https://doi.org/10.1016/j.jcat.2008.07.020.
[54] P. Li, K.A. Perreau, E. Covington, C.H. Song, G.R. Carmichael, V.H. Grassian, J. Geophys. Res. Atmos. 106 (2001) 5517–5529, https://doi.org/10.1029/2000JD900573.
[55] A.M. Hernández-Giménez, J. Ruiz-Martínez, B. Puértolas, J. Pérez-Ramírez, P.C.A. Bruijnincx, B.M. Weckhuysen, Top. Catal. 60 (2017) 1522–1536, https://doi.org/10.1007/s11244-017-0836-7.
[56] S. Carlos-Cuellar, P. Li, A.P. Christensen, B.J. Krueger, C. Burrichter, V.H. Grassian, J. Phys. Chem. A 107 (2003) 4250–4261, https://doi.org/10.1021/jp0267609.
[57] M. Waqif, O. Saur, J.C. Lavalley, J. Wang, B.A. Morrow, Appl. Catal. 71 (1991) 319–331, https://doi.org/10.1016/0166-9834(91)85089-E.
[58] M. Bensitel, M. Waqif, O. Saur, J.C. Lavalley, J. Phys. Chem. 93 (1989) 6581–6582, https://doi.org/10.1021/j100355a003.
[59] V. Crocella, G. Cerrato, G. Magnacca, C. Morterra, F. Cavani, L. Maselli, S. Passeri, Dalton Trans. 39 (2010) 8527–8537, https://doi.org/10.1039/C002490B.
[60] J.-C. Lavalley, J. Lamotte, V. Lorenzelli, J. Chem. Soc. Chem. Commun. (1985) 1006–1007, https://doi.org/10.1039/C39850001006.
[61] E. Finocchio, G. Busca, V. Lorenzelli, R.J. Willey, J. Chem. Soc. Faraday Trans. 90 (1994) 10, https://doi.org/10.1039/FT9949003347.
[62] J. Quiroz, J.-M. Giraudon, A. Gervasini, C. Dujardin, C. Lancelot, M. Trentesaux, J.-F. Lamonier, ACS Catal. 5 (2015) 2260–2269, https://doi.org/10.1021/cs501879j.
[63] X.D. Peng, M.A. Barteau, Langmuir 5 (1989) 1051–1056, https://doi.org/10.1021/la00088a031.
[64] C. Resini, S. Cavallaro, F. Frusteri, S. Freni, G. Busca, React Kinet Catal Lett 90 (2007) 117–126, https://doi.org/10.1007/s11144-007-5027-2.
[65] H. Härelind, F. Gunnarsson, S.M.S. Vaghefi, M. Skoglundh, P.-A. Carlsson, ACS Catal. 2 (2012) 1615–1623, https://doi.org/10.1021/cs3001754.
[66] Zs. Ferencz, A. Erdőhelyi, K. Baán, A. Oszkó, L. Óvári, Z. Kónya, C. Papp, H.-P. Steinrück, J. Kiss, ACS Catal. 4 (2014) 1205–1218, https://doi.org/10.1021/cs500045z.
[67] J.E. Rekoske, M.A. Barteau, Langmuir 15 (1999) 2061–2070, https://doi.org/10.1021/la9805140.
[68] J.E. Bailie, C.H. Rochester, G.J. Hutchings, Faraday Trans. 93 (1997) 4389–4394, https://doi.org/10.1039/a704791f.
[69] S.R. Tong, L.Y. Wu, M.F. Ge, W.G. Wang, Z.F. Pu, Atmos. Chem. Phys. 10 (2010) 7561–7574, https://doi.org/10.5194/acp-10-7561-2010.